Hindawi
Shock and Vibration
Volume 2019, Article ID 6283765, 11 pages
https://doi.org/10.1155/2019/6283765

Research Article

Experimental Research on the Impact Environment of Multiplate Cabinet

Jun Guo,[1] **Shizhang Huang**,[1] **Youwei Kang**,[2] **Ning Hao**,[1] **and Hao Xie**[1]

[1]*College of Shipbuilding Engineering, Harbin Engineering University, Harbin 150001, China*
[2]*CIMC Offshore Co.Ltd., Shenzhen 518052, China*

Correspondence should be addressed to Jun Guo; guo_jun@hrbeu.edu.cn

Received 12 September 2018; Revised 16 November 2018; Accepted 26 November 2018; Published 3 January 2019

Academic Editor: Marco Gherlone

As an installation and protection device for electrical and electronic components, a shipboard cabinet is a typical multiplate structure. In order to study the impact environment distribution laws of such structures, impact testing was carried out on a shipboard cabinet under four working conditions in this paper. In addition, the impact response characteristics of such a multiplate structure were determined by numerical simulation and theoretical analysis. The impact environments of some pivotal points in cabinet were measured and some laws of dynamic response were found. The impact environment of central position was more severe on a single plate because of the first vibration modal. For different plates, the responses were usually similar at low-frequency band and a little different at high-frequency band. The theoretical analysis of the single degree of freedom oscillator was carried out, and the sensitivity of the response to the different characteristic frequencies was discussed based on the shock spectrum theory. A new method of calculating the response at a special frequency was proposed and verified.

1. Introduction

With the development of various antiship weapons, a ship's ability to resist load impact is becoming more and more important in the research of battleships' viability [1, 2]. How to ensure the normal operation of the key subsystems of ships is a major task in the research of modern battleships. The electronic system is like a "nerve and blood circulation system" for transmitting signals and energy in a ship, so its impact resistance is very important. However, electrical and electronic devices usually are characterized by structural precision and extremely sensitive to underwater explosion. When subjected to explosion impact, they may tend to turn-off or produce plastic deformation to affect the reliability of equipment and endanger the safety of ships. At present, the most researchers focus on the mechanical equipment, such as diesel engine and gearbox [3, 4]. The electric equipment was not paid enough attention. Therefore, the current research on this area is relatively less and the experimental data are especially rare. In 1988, the mechanical characteristics of electronic cabinets, printed circuit boards, and electronic components were systematically analyzed and studied by Steinberg [5], which was regarded as one of the theoretical pillars of the dynamic characteristics of electronic equipment. The failure modes of electric equipment are various. For reed contact switches, higher-frequency impact loads are more likely to cause violent contact chatter and broken circuit, while lower frequency impact loads cause the larger stress and plastic deformation at the root of reeds [6]. For printed circuit board, the results of drop test and numerical simulation demonstrate that the mechanical shock causes multiple bending or vibration which induces the solder joint fatigue failure [7–9]. Besides, in the previous drop test, it was difficult to meet the requirements of accurate description of the impact input. Therefore, with the wide using of electric equipment, studying the cabinet is of great significance.

As a typical frame structure, the multiplate cabinet provides impact protection for its internal electric equipment to ensure their normal working. The impact environment in cabinet is closely related to the impact resistance

of electronic components and has some specific rules. Since the scale of electronic devices is far less than the scale of cabinet plates, different electronic components in different plates and different positions may experience different impact environments. Shen [10] qualitatively analyzed the vibration isolation and buffer design of the ship cast aluminum closed cabinet and determined the vibration isolation and buffer system of the cabinet with a contrast test. Huang [11] used topology optimization combined with vibration shock tests to select the vibration isolation and buffer system of the cabinet. Blast loading response of lattice structures was studied numerically and experimentally [12]. In addition, an experimental study of frequency and time domain identification algorithms was presented and their effectiveness in structural health monitoring of frame structures was discussed [13]. Plates are main parts of cabinets, and their dynamic responses have attracted wide attention [14–18]. However, all of the aforementioned researches focused on the strength of cabinet or dynamic responses of isolated plates, but ignored the fact that the internal impact environment of a shipboard cabinet is very complex. The distribution law and values of impact environment in cabinet are most important for electronic equipment installed in the cabinet.

Considering the above, this paper provides a shock test method for shipboard equipment, and the data obtained can be directly used as the impact input for ship-borne electrical equipment. This paper took a shipboard cabinet as the research object and used the impact machine as the loading equipment. The experiments were conducted under four different working conditions, and the impact environment distributions were obtained. At the same time, the impact environment of the electrical equipment of the cabinet was obtained via finite element simulation. This paper provides not only a reference for the research of the impact environment of such frame structure but also the basis for the installation and protection of the ship electrical equipment.

2. Impact Experiment of Shipboard Cabinet

2.1. Experimental Method. In this paper, a shipboard cabinet was used as the experimental research object. Some electrical components such as control circuit, IGBT component, capacitance, inductance, transformer, and relay were fixed on the cabinet plates by bolts. The electronic cabinet was a frame structure composed of a main frame, front panel, and rear panel. The geometry of the shipboard cabinet is shown in Figure 1, and the corresponding dimensions are shown in Table 1. The whole cabinet is made up of Q235 steel which has a density of 7800 kg/m^3, Young's modulus of 2.1e11 Pa, and Poisson's ratio of 0.3. The experimental reject was installed on the 500 kg double-wave impact test machine. Four transverse plates' thickness is 1.0 mm, and three vertical plates' thickness is 1.5 mm.

When testing, the accumulator produced a great power and force impact hammer to move upward. The impact hammer hit on impact table and gave a shock to testing equipment. The applied loads were half sine waves. The buffer cylinder was used to control strength of the loads. Twelve measuring points were chosen, among which 2 points were arranged on the bench table diagonally, 5 points on the bottom plate, and the other 5 on the upside plate. Acceleration sensors were stacked at these 12 points. The whole experimental method is shown in Figure 1, and the physical experimental layout is shown in Figure 2.

According to the experimental requirements of the national military standard GJB1060.1-91 [19], the electronic cabinet was rigidly mounted on the impact machine table through the auxiliary panel. In this paper, the impact experiment was carried out on the electronic cabinet under four different working conditions The impact velocity of the impact table was changed by storing different energy of the energy storage device of the impact test machine, and the relative velocities of the four working conditions were 1.9 m/s, 3.2 m/s, 4 m/s, and 4.8 m/s. Generally speaking, the spectrum velocities of impact environment in warship will not exceed 5 m/s; the four working conditions selected in this paper cover most of the possible loads of shipboard equipment and have a great degree of differentiation.

The spectrum velocity method is usually used to represent the destructive potential of impact [20]. At present, the impact spectrum is widely used to describe the impact environment in the study of the impact resistance of submarines and surface ship equipment. It is mainly used to evaluate the possibility of equipment failure and to establish the design spectrum of equipment assessment. With the continuous improvement of the calculation method for impact response spectrum analysis, the impact response spectrum analysis has gradually become an effective method to solve the problem of vibration and impact. In this paper, the time signal of different positions was transformed into the velocity spectrum by the recursive algorithm [21, 22]. The damping coefficient was selected to be 0.05, sampling frequency was 25 kHz, and the original data were not filtered.

It is shown in Figure 3 that both the curves of acceleration with time and shock spectrums of two measuring points located at the positive ends of the diagonal line on the impact table were very similar. Therefore, the impact environment of every point on the impact table seemed to be the same. It means the impact environment of any point on the table can be used as the load of the impact experiment and numerical simulation under a given working condition.

2.2. Numerical Verification. For verifying the reliability of the experimental data, an impact simulation was carried out. As shown in Figure 4, an infinite model of the shipboard cabinet was established with solid elements and loaded with the changing acceleration under working condition 1 below the bottom plate. The experimental and numerical results of the central position on the bottom plate were compared. It is seen in Figure 5 that the shock spectrums extracted from measuring point 7 of the experiment and numerical simulation were very similar under the same working condition. Thus, the reliability of experiment was verified.

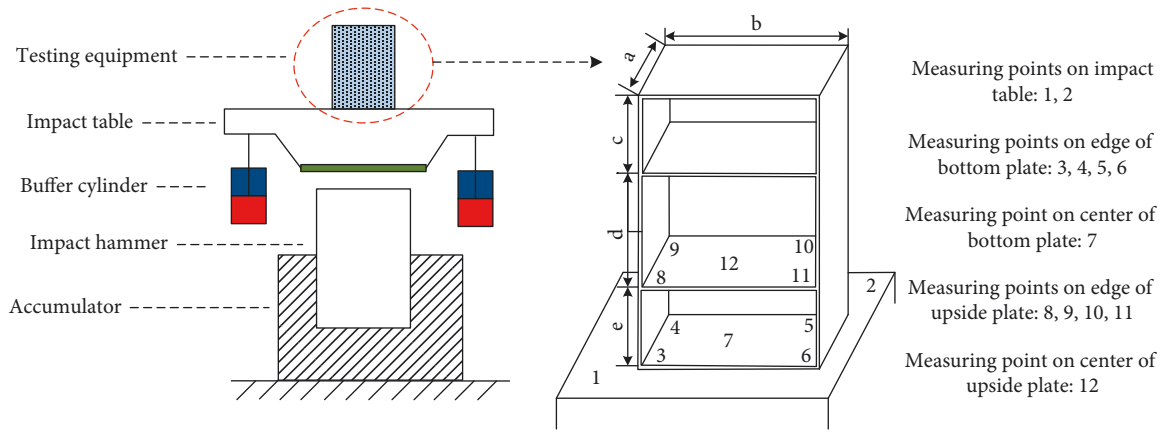

Figure 1: Programmer of the impact experiment.

Table 1: Size of the shipboard cabinet.

Length(mm)	a	b	c	d	e
	400	500	330	430	240

3. Impact Environments of the Single Plate

For exploring the difference of impact environments from edge measuring points to central measuring points, the acceleration curves are compared and shown in Figures 6 and 7.

As is shown in the above figures, the acceleration response of each point in the cabinet shows exponential decay trend. For the bottom plate, there exist many large peaks in the curve of central point. But for the upside plate, there was no obvious difference between the edge measuring points and the central point. That is because the upside plate can be seen as a whole when impact load is transmitted to upside plate. In order to explain the relationship of dynamic response and frequency, the shock spectrums of measuring points are given in Figures 8 and 9.

As seen in Figures 8 and 9, for the bottom plate, no matter how the working condition is, the impact environments of four edge measuring points are basically the same and obviously smaller than the impact environment of the central point. This phenomenon can be explained according to the nature vibration characteristics of plates. The central point is the node of first modal shape, so its vibration is much easier to be inspired and more drastic. Above results provide an engineering suggestion that the electronic equipment with poor shock resistance should be installed at edges of plate, and the equipment with good shock resistance can be installed at the center.

4. Impact Environments of the Different Plates

4.1. Experimental Results. Not only the impact environment from edge to center in single plate, but also the difference of impact environments of different plates was explored in this paper. The impact environments of measuring points 1, 7, and 12 are compared under four working conditions in Figure 10.

Figure 10 shows that the impact environments of the upside center and the bottom center were very close at the low-frequency band. The cross sectional size is smaller than height of the cabinet. So, the whole cabinet can be treated as a pole and its natural longitudinal vibrating frequency is much bigger than the vibration frequencies of plates. The difference of impact environments of measuring points 7, 12 under four working conditions is mainly existing in the middle frequency band. That may be influenced by the vibration frequencies of plates. When the frequency of the load approaches the first vibration frequency of the plate, there will be a phenomenon of excessive local response. Therefore, it was worthy being discussed how the frequency of load influence cabinet's dynamic response.

4.2. Simulation Results. In order to explore the difference of shock responses of plates, Figure 11 shows a numerical model of a multiplate installation structure established by shell elements. The model was a 500 × 400 × 1200 mm cabinet, and the distances between every two adjacent plates were the same. The input loads were loaded at the bottom and transmitted to the top plate. The dynamic impact response characteristics of mechanical equipment are closely related to their natural vibration characteristics [23–26]. Modal analysis results show that the first-order frequencies of the local vibration from the first plate to the fifth plate in the model were 50 Hz, 60 Hz, 68 Hz, 78 Hz, and 90 Hz, respectively.

The responses of all plates are shown in Figure 12. For each curve in Figure 12, there exist at least 2 peaks. The first peak was caused by the frequency of impact load. The second peak stands for first natural vibration frequency of plate. When the frequency of input load was much smaller than the vibration frequency of any plate in cabinet, no matter how the amplitude of load is, the impact environments of all plates were basically same at the low-frequency band and a little different at the high-frequency band. Each shock spectrum curve has two crests, and they are located at frequency of load and plate's first vibration frequency. The

Figure 2: Arrangement of the impact experiment. (a) Measuring points on the impact table. (b) Measuring points in the cabinet.

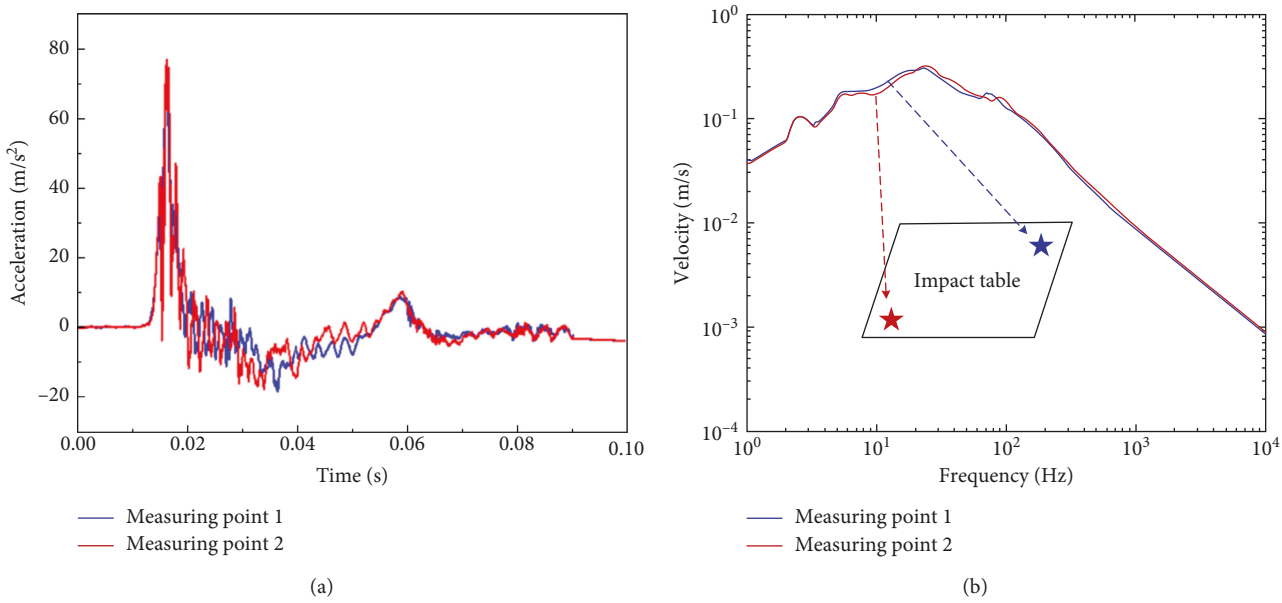

Figure 3: Comparison of measuring points 1 and 2 under working condition 1. (a) Acceleration curves with of measuring points 1 and 2. (b) Shock spectrums of measuring points 1 and 2.

little difference can be ignored in engineering application. However, when the frequency of load is being close to the first vibration frequency of plate; for example, the frequency of load is 40 Hz and the minimum frequency of plates is 50 Hz, the results changed.

It can be seen from Figure 13 that when the frequency of impact input was 40 Hz, the response of all of the plates in the cabinet appeared to be distinct, and the maximum response attenuated from the bottom plate to the top plate. The aforementioned phenomenon followed some rules. When the frequency of load is far away from the frequencies of plates, the impact environments of different plates are the same. When the frequency of load is close to the frequencies of plates, the impact environment of the plate whose vibration frequency is most close to the frequency of load is most severe.

5. Response of the Plate at a Specific Frequency

5.1. Theoretical Analysis. In general, the electronic component installed on plate (Figure 14) is sensitive to load with several specific frequencies. When the frequency of

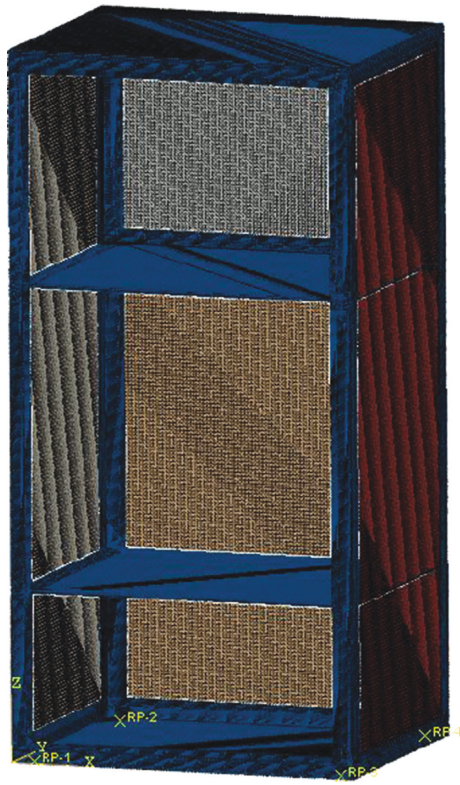

Figure 4: Finite element model of shipboard cabinet.

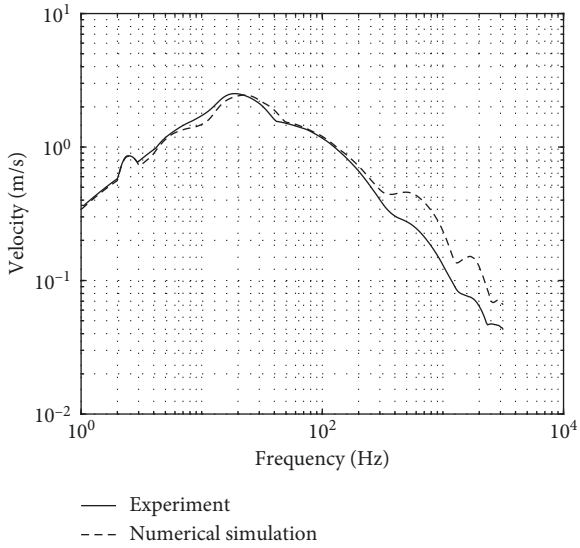

Figure 5: The results comparison of numerical simulation and experiment.

load is close to the components' natural vibration frequencies, the resonance may occur and cause damage. The response of the plate is also the load of the electronic components. Therefore, in order to provide reference for the design and antiimpact protection of electronic equipment, this paper presents a new method to estimate shock response of the plate's center at the specific frequency.

In this paper, the central position of the plate was simplified as a single degree of freedom system and was loaded with a sine wave of $\ddot{u}(\tau)$:

$$\ddot{u}(\tau) = A \sin \omega_i \tau, \tag{1}$$

where A is amplitude and ω_i is frequency.

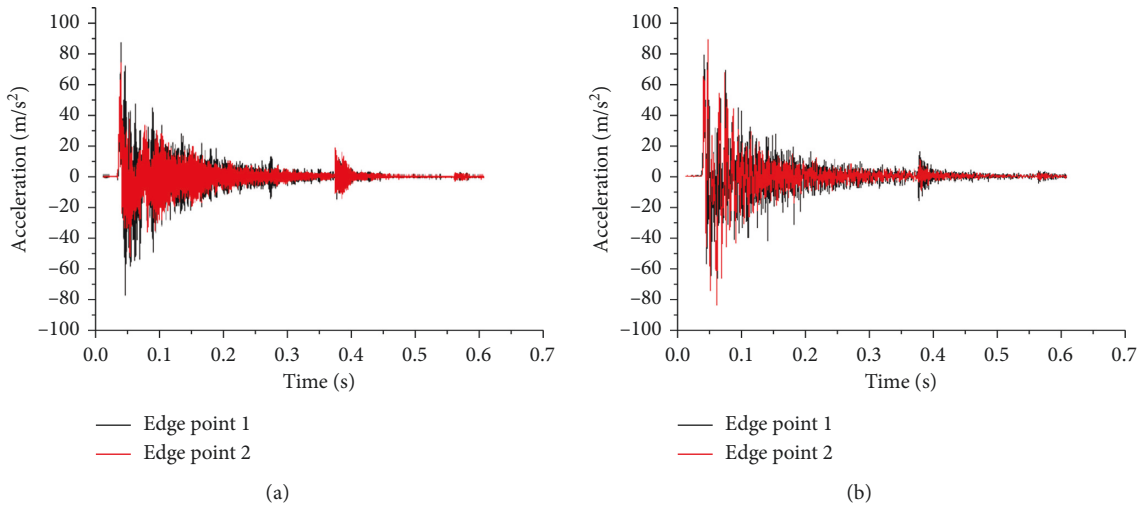

Figure 6: Acceleration curves of edge points under working condition 1. (a) Bottom plate. (b) Upside plate.

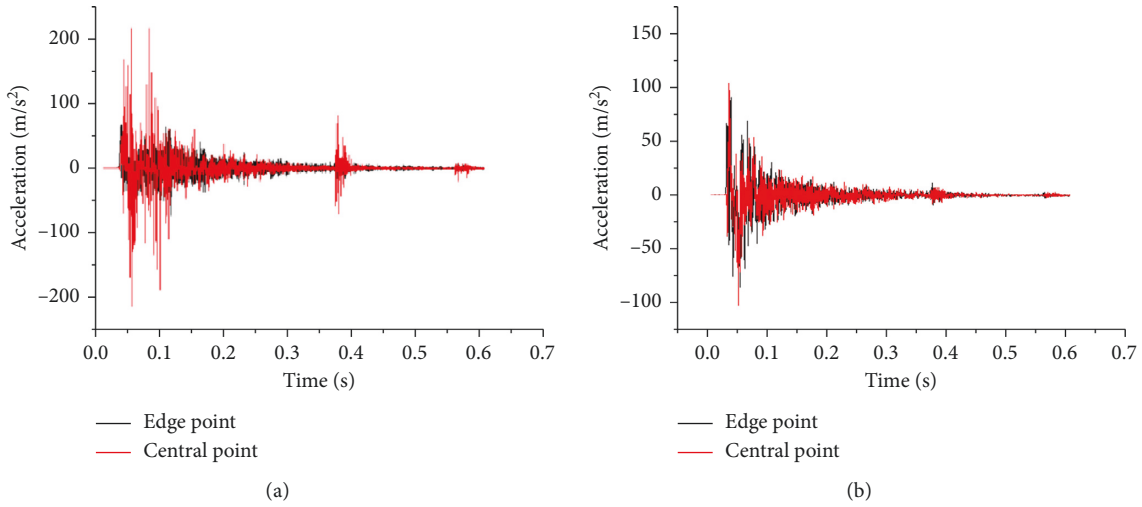

Figure 7: Acceleration curves of edge point and central point under working condition 1. (a) Bottom plate. (b) Upside plate.

The shock spectrums are shown in Figure 15. When the load is $\ddot{u}_0(\tau)$ whose amplitude is A_0 and frequency is f_0, the maximum response of the system was V_{00}. When the load is $\ddot{u}_1(\tau)$ whose amplitude is A_i and frequency is f_i, the response at f_0 was V_{0i}. The relationship between V_{00} and V_{0i} should be discussed.

According to the computing method of shock response spectrum, the spectrum displacement can be obtained by Duhamel integration, thus,

$$\delta_i(t) = -\frac{1}{\omega_d\sqrt{1-\xi^2}}\int_0^t \ddot{u}(\tau)e^{-\xi\omega_0(t-\tau)} \cdot \sin\left[\omega_d\sqrt{1-\xi^2}\,(t-\tau)\right]d\tau, \quad (2)$$

where $\delta_i(t)$ is the spectrum displacement; ω_d is natural frequency; ξ is damping; and ω_0 is frequency of load.

For the undamped system, $\xi = 0$, so

$$\begin{aligned}\delta_i(t) &= -\frac{1}{\omega_d}\int_0^t A_i \sin\omega_i\tau \sin\left[\omega_d(t-\tau)\right]d\tau,\\ \delta_i(t) &= -\frac{A_i}{\omega_d}\int_0^t \{\cos\left[(\omega_i+\omega_d)\tau-\omega_d t\right]\\ &\quad -\cos\left[(\omega_i-\omega_d)\tau+\omega_d t\right]\}d\tau, \quad (3)\\ \delta_i(t) &= -\frac{A_i}{\omega_d}\left[\left(\frac{1}{\omega_i+\omega_d}-\frac{1}{\omega_i-\omega_d}\right)\sin\omega_i t\right.\\ &\quad \left.+\left(\frac{1}{\omega_i+\omega_d}+\frac{1}{\omega_i-\omega_d}\right)\sin\omega_d t\right].\end{aligned}$$

Thus, the spectrum velocities were gained

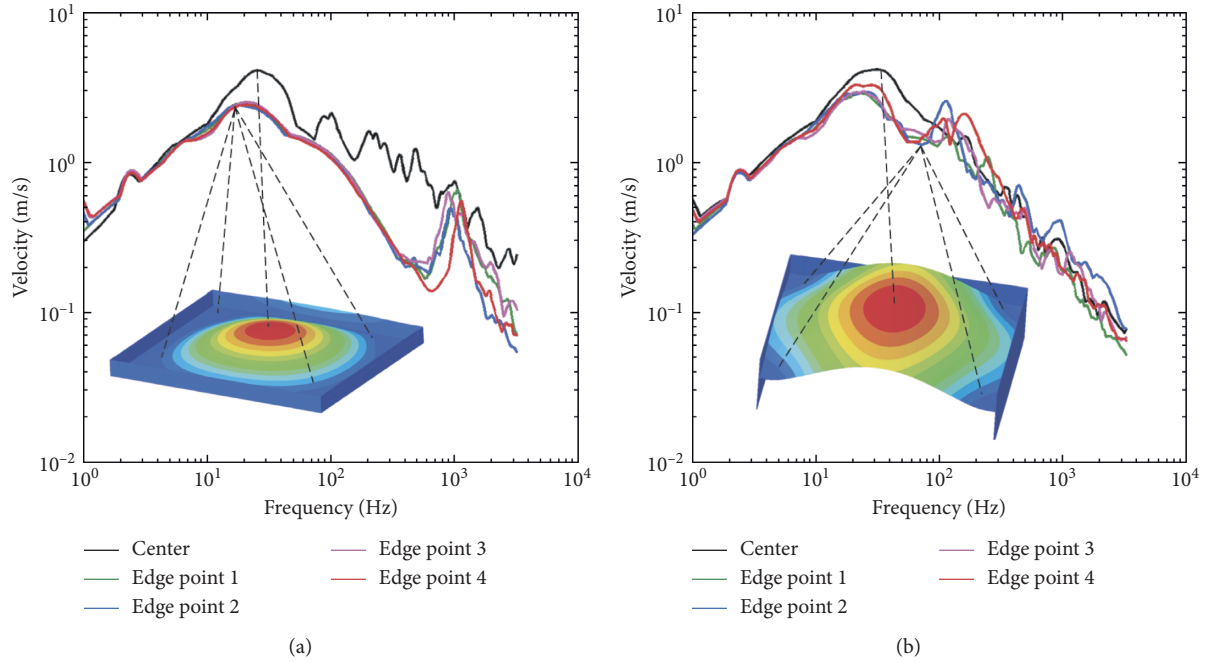

Figure 8: Impact environment in the single plate under working condition 1. (a) Bottom plate. (b) Upside plate.

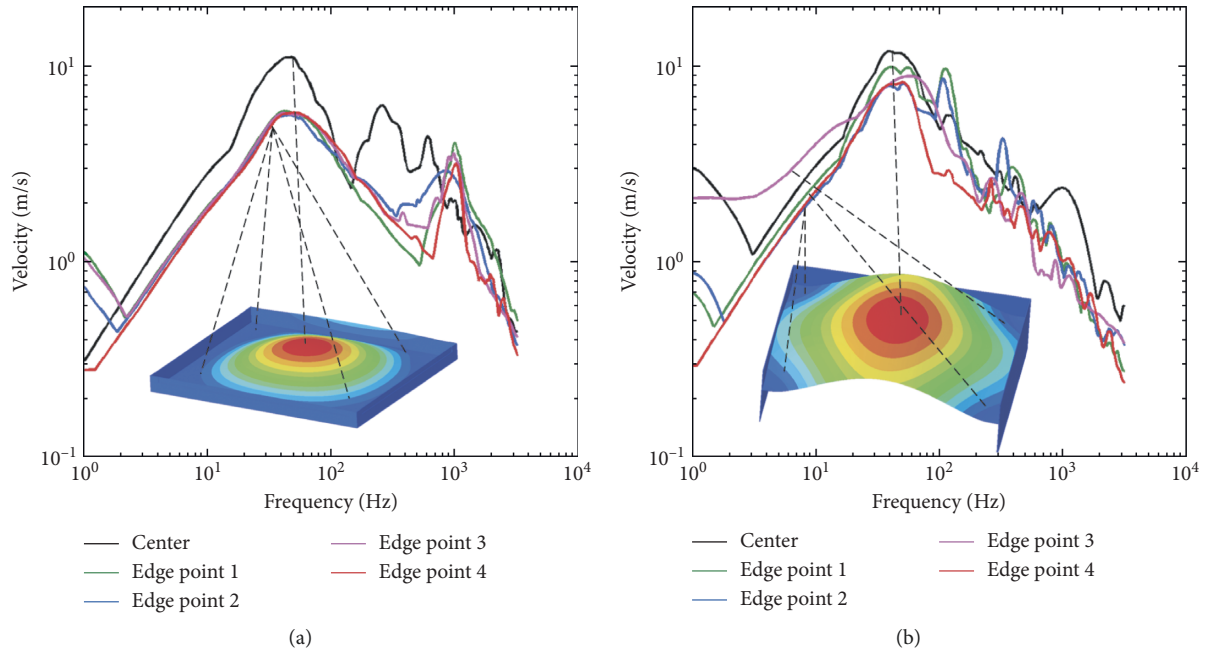

Figure 9: Impact environment in the single plate under working condition 2. (a) Bottom plate. (b) Upside plate.

$$D = \max|\delta_i(t)| = \left| -\frac{1}{\omega_d} \int_0^t A \sin \omega_i \tau \sin[\omega_d (t-\tau)] d\tau \right|,$$

$$V_0 = \omega_0 D = 2\pi f_0 \cdot \max|\delta(t)|. \tag{4}$$

This paper defines β to describe ratio of V_{0i} to V_{00}.

$$\beta = \frac{V_{0i}}{V_{00}} = \frac{2\pi f_0 \left| -(1/\omega_d) \int_0^t A_i \sin \omega_i \tau \sin[\omega_d (t-\tau)] d\tau \right|}{2\pi f_0 \left| -(1/\omega_d) \int_0^t A_0 \sin \omega_0 \tau \sin[\omega_d (t-\tau)] d\tau \right|}. \tag{5}$$

Therefore, β is a function of f_i/f_0, A_i/A_0 and ω_d.

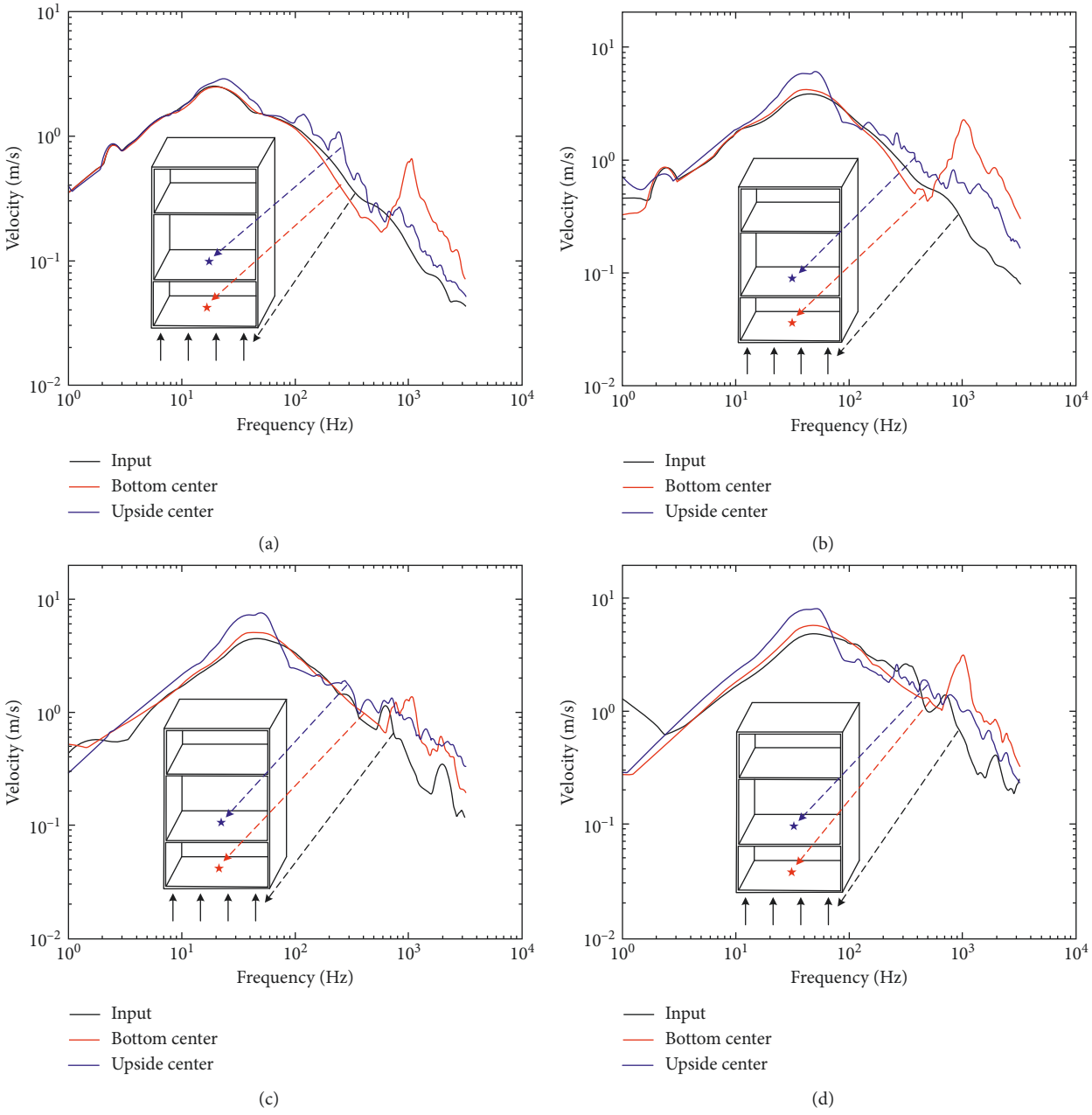

Figure 10: Impact environments of different plates under four working conditions. (a) Working condition 1. (b) Working condition 2. (c) Working condition 3. (d) Working condition 4.

$$\beta = F\left(\frac{f_i}{f_0}, \frac{A_i}{A_0}, \omega_d\right),$$
$$\beta = \frac{A_i}{A_0}\frac{\omega_i}{\omega_0}\sqrt{\left(\frac{\omega_i^2+\omega_d^2}{\omega_0^2+\omega_d^2}\right)\left(\frac{\omega_0^2-\omega_d^2}{\omega_i 2-\omega_d^2}\right)}. \quad (6)$$

When $A_i = A_0$, ω_1, $\omega_0 \neq \omega_d$, and ω_d is 40 Hz, the relationship between β and f_i/f_0 can be seen in Figure 16. Four curves representing f_0 was 20 Hz, 30 Hz, 50 Hz, and 60 Hz.

Actually, the load usually is an irregular wave and can be seen as a composition of infinite sine waves. In this paper, for reducing the computation cost, it was decomposed to 10 sine waves by the empirical mode decomposition method [27–29]. Frequencies of these sine waves were $f_1, f_2, \ldots f_n$. There exists a certain β corresponding to every sine wave. The response at f_i of the plate was described as a nonlinear combination of β_i and f_i.

$$V_i = H_i(\beta_1 \cdot f_1 + \beta_2 \cdot f_2 + \ldots + 1 \cdot f_i + \ldots + \beta_n \cdot f_n) = H_i \sum_{i=1}^{n} \beta_i f_i. \quad (7)$$

5.2. Comparison of Experimental Results with Theoretical Results. In order to prove the theoretical analysis, a comparison of values obtained by the two methods was carried out and the error is shown in Table 2.

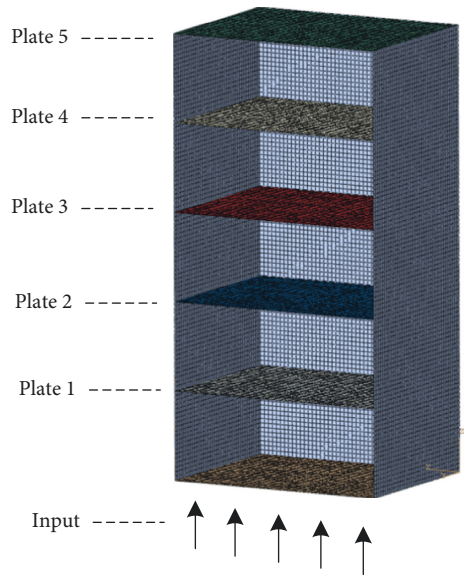

Figure 11: Model of multiplates frame structure.

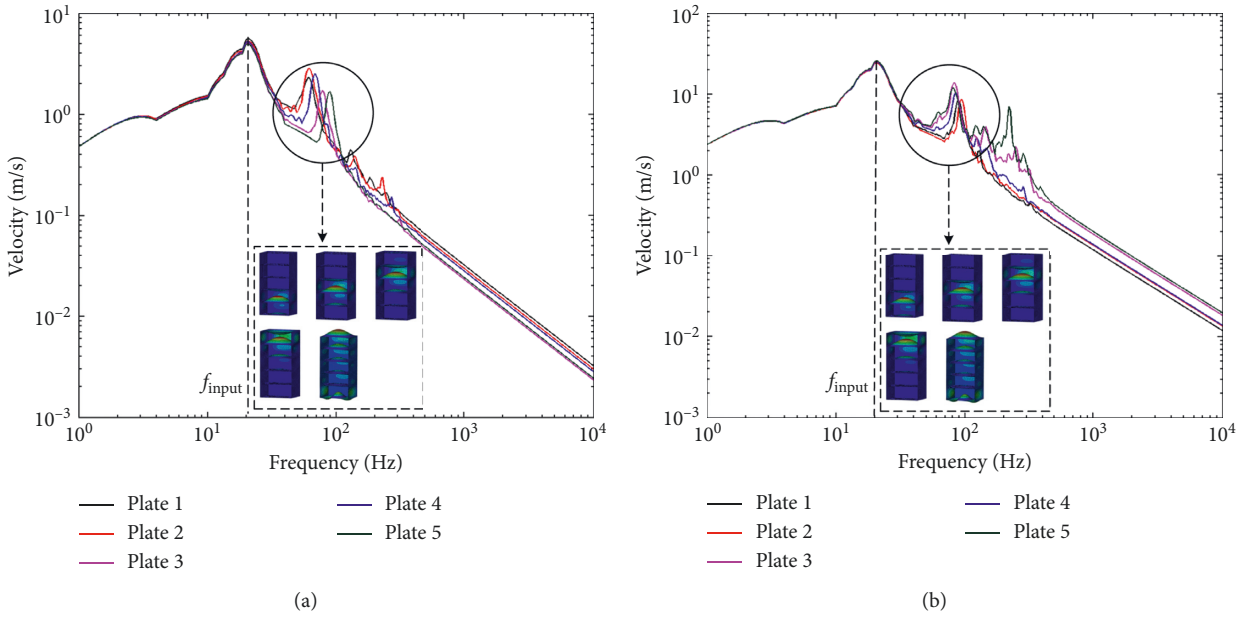

Figure 12: Shock spectrums of five plates when frequency of load is 20 Hz. (a) Load with low amplitude. (b) Load with high amplitude.

From Table 2, all of the errors under four working conditions were smaller than 20% and permitted, so the feasibility of the new method was verified. The error was resulted due to three reasons: the plate was not totally equal to a single degree of freedom system, some error was caused during the impact experiment, and the input loading was not decomposed enough.

6. Conclusions

For the purpose of providing impact input for electronic equipment, the impact environment of each plate in the cabinet was analyzed based on the impact experiment and numerical simulation of a certain type of warship cabinet. The following conclusions were drawn.

(1) For the bottom plate, no matter how the load is, the impact environment of center on plate is obviously more severe. But for the upside plate, the impact environments of edge points and central point are basically the same.

(2) In the cabinet, when the frequency of load is far away from the frequencies of plates, the impact environments of different plates are the same. When the frequency of load is close to the frequencies of plates,

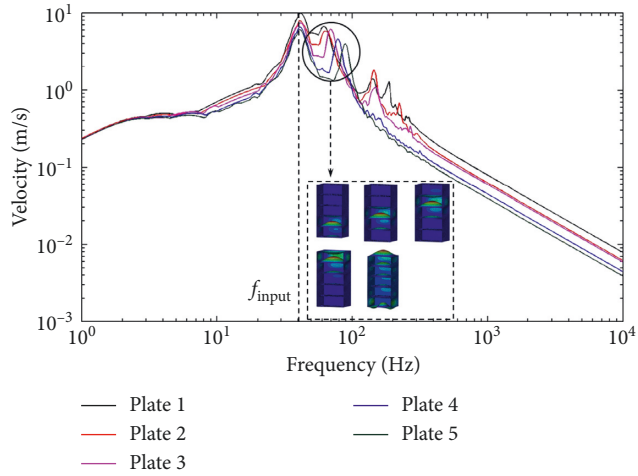

Figure 13: Shock spectrums of five plates when frequency of loads is 40 Hz.

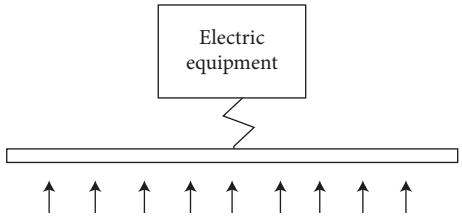

Figure 14: The plate and electric equipment.

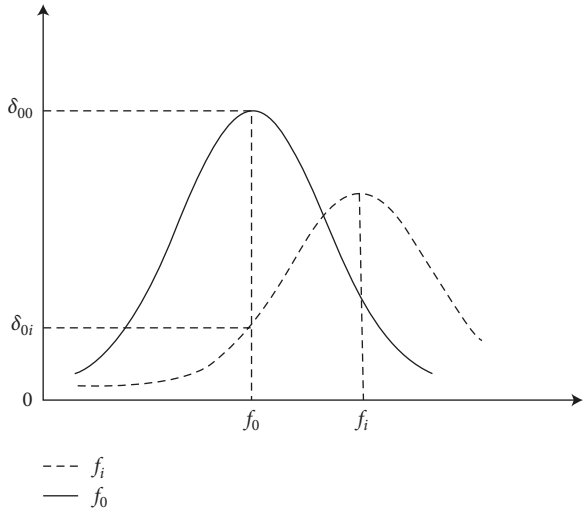

Figure 15: Response at same specific frequency under different loads.

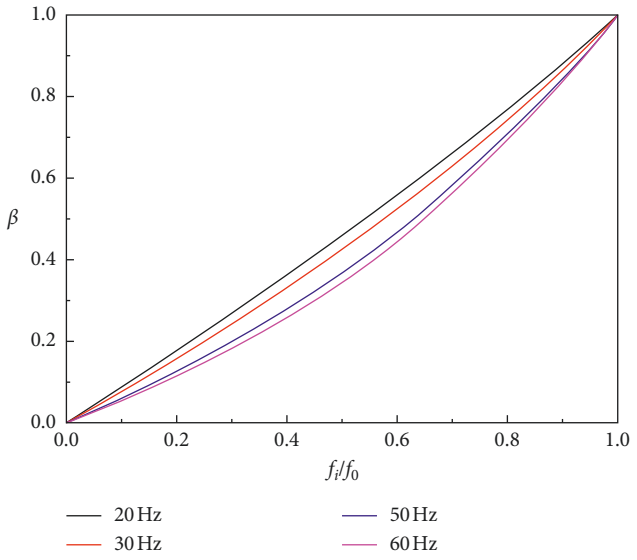

Figure 16: The curve of β with f_i/f_0.

Table 2: Comparison and error of spectrum velocities.

Working condition	1	2	3	4
Experimental value (m/s)	3.65	5.34	7.95	10.84
Theoretical value (m/s)	3.24	4.68	6.54	8.98
Error (%)	11.2	12.4	17.7	17.2

the impact environment of the plate whose vibration frequency is most close to frequency of load is most severe. Therefore, when assessing such electrical components, the location should be considered along with the frequency of load.

(3) The theoretical analysis of the single degree of freedom oscillator is carried out, and the sensitivity of the response to the different frequencies of load is discussed based on the shock spectrum theory. A new method of calculating the response at the special frequency of plate is proposed and verified.

Data Availability

The data used to support the findings of this study are included within the article.

Conflicts of Interest

The authors declare that they have no conflicts of interest.

Acknowledgments

This study was funded by "Special Fund of the Ministry of Industry and Information Technology, China (No. 2018287)."

References

[1] A.-M. Zhang, Y. Wen-Shan, and Y. Xiong-Liang, "Numerical simulation of underwater contact explosion," *Applied Ocean Research*, vol. 34, pp. 10–20, 2012.

[2] H. Cheng, A. M. Zhang, F. R. Ming et al., "Study on coupled dynamics of ship and flooding water based on experimental and SPH methods," *Physics of Fluids*, vol. 29, no. 10, article 107101, 2017.

[3] J. Wang, "Response analysis of shipboard equipment under different underwater explosion environment," *Journal of Vibration and Shock*, vol. 34, no. 15, pp. 181–187, 2015, in Chinese.

[4] L. Feng, "Reliability analysis for shock resistance ability of shipboard equipments," *Journal of Vibration and Shock*, vol. 32, no. 1, pp. 140–144, 2013, in Chinese.

[5] D. Steinberg, *Vibration Analysis of Electronic Systems*, John Wiley and Son's, New York, NY, USA, 1988.

[6] M. Yan, "Shock response analysis for reed contact switches in naval ships' electrical equipment," *Journal of Vibration and Shock*, vol. 35, no. 1, pp. 183–187, 2016, in Chinese.

[7] Y. Q. Wang, K. H. Low, F. X. Che et al., "Modeling and simulation of printed circuit board drop test," in *Proceedings of 5th Electronics Packaging Technology Conference (EPTC 2003)*, pp. 263–268, Pan Pacific Hotel, Singapore, December 2003.

[8] Y. T. Tong, L. Jing-en, P. Eric et al., "Novel numerical and experimental analysis of dynamic responses under board level drop test[A]," in *Proceedings of 5th International Conference on Thermal and Mechanical Simulation and Experiments in Micro-Electronics and Micro-Systems[C]*, pp. 133–140, Cascais, Portugal, April 2004.

[9] J. Gu, C. T. Lim, and A. A. O. Tay, "Modeling of solder joint failure due to PCB bending during drop impact," in *Proceedings of 6th Electronics Packaging Technology Conference (EPTC 2004)*, pp. 678–683, Pan Pacific Hotel, Singapore, December 2004.

[10] W. Shen, "The analysis about vibration and shock of a plug-in classis in electronic cabinet," *Shock and Vibration*, vol. 21, no. 6, 2005, in Chinese.

[11] G. Huang, "Optimized design of marine cabinet of resisting strong impact," *Electro-Mechanical Engineering*, vol. 26, no. 1, 2010, in Chinese.

[12] S. McKown, Y. Shen, W. K. Brookes et al., "The quasi-static and blast loading response of lattice structures," *International Journal of Impact Engineering*, vol. 35, no. 8, pp. 795–810, 2008.

[13] G. Fraraccio, A. Brugger, and R. Betti, "Experimental studies on damage detection in frame structures using vibration measurements," *Shock and Vibration*, vol. 17, no. 6, pp. 697–721, 2015.

[14] J. Liu, S. Pattofatto, D. Fang, F. Lu, and H. Zhao, "Impact strength enhancement of aluminum tetrahedral lattice truss core structures," *International Journal of Impact Engineering*, vol. 79, pp. 3–13, 2015.

[15] V. Aune, G. Valsamos, F. Casadei, M. Larcher, M. Langseth, and T. Børvik, "Numerical study on the structural response of blast-loaded thin aluminium and steel plates," *International Journal of Impact Engineering*, vol. 99, pp. 131–144, 2017.

[16] V. Aune, G. Valsamos, F. Casadei et al., "On the dynamic response of blast-loaded steel plates with and without preformed holes," *International Journal of Impact Engineering*, vol. 108, pp. 27–46, 2017.

[17] N. Jacob, C. Kim, S. Yuen et al., "Scaling aspects of quadrangular plates subjected to localised blast loads-experiments and predictions," *International Journal of Impact Engineering*, vol. 30, no. 8-9, pp. 1179–1208, 2004.

[18] C. F. Hung, P. Y. Hsu, and J. J. Hwang-Fuu, "Elastic shock response of an air-backed plate to underwater explosion," *International Journal of Impact Engineering*, vol. 31, no. 2, pp. 151–168, 2005.

[19] J. E. Alexander, "Shock response spectrum-A primer," *Sound and Vibration*, vol. 43, pp. 6–14, 2009.

[20] GJB1060.1-91, *General Requirement for Environmental Conditions of Naval Ships Mechanical Environments*, Industry Committee of National Defense Science and Technology, Beijing, China, 1991, in Chinese.

[21] H. A. Gaberson, *Pseudo Velocity Shock Spectrum Rules for Analysis of Mechanical Shock*, Shock and Vibration, Orlando, FL, USA, 2007.

[22] J. N. Martin and A. J. Sinclair, "On the shock-response-spectrum recursive algorithm of Kelly and Richman," *Shock and Vibration*, vol. 19, no. 1, pp. 19–24, 2012.

[23] H. Li, F. Pang, X. Wang, Y. Du, and H. Chen, "Free vibration analysis of uniform and stepped combined paraboloidal, cylindrical and spherical shells with arbitrary boundary conditions," *International Journal of Mechanical Sciences*, vol. 145, pp. 64–82, 2018.

[24] H. Li, F. Pang, X. Miao, Y. Du, and H. Tian, "A semi-analytical method for vibration analysis of stepped doubly-curved shells of revolution with arbitrary boundary conditions," *Thin-Walled Structures*, vol. 129, pp. 125–144, 2018.

[25] H. Li, F. Pang, X. Wang et al., "Free vibration analysis for composite laminated doubly-curved shells of revolution by a semi analytical Method," *Composite Structures*, vol. 201, pp. 86–111, 2018.

[26] F. Pang, H. Li, X. Wang, X. Miao, and S. Li, "A semi analytical method for the free vibration of doubly-curved shells of revolution," *Computers and Mathematics with Applications*, vol. 75, no. 9, pp. 3249–3268, 2018.

[27] P. Flandrin, G. Rilling, and P. Goncalves, "Empirical mode decomposition as a filter bank," *IEEE Signal Processing Letters*, vol. 11, no. 2, pp. 112–114, 2004.

[28] K. Dragomiretskiy and D. Zosso, "Variational mode decomposition," *IEEE Transactions on Signal Processing*, vol. 62, no. 3, pp. 531–544, 2014.

[29] N. E. Huang, Z. Shen, S. R. Long et al., "The empirical mode decomposition and the Hilbert spectrum for nonlinear and non-stationary time series analysis," *Proceedings of the Royal Society A: Mathematical, Physical and Engineering Sciences*, vol. 454, no. 1971, pp. 903–995, 1998.